Virchows Arch (1998) 433:41–48

ORIGINAL ARTICLE

Tarou Irié · Jun Cheng · Shin Kimura
Ryuichi Munakata · Shuhzou Taira · Takashi Saku

Intracellular transport of basement membrane-type heparan sulphate proteoglycan in adenoid cystic carcinoma cells of salivary gland origin: an immunoelectron microscopic study

Received: 2 July 1997 / Accepted: 19 February 1998

Abstract ACC3, a human adenoid cystic carcinoma cell system of salivary gland origin, is able to synthesize and secrete a large amount of basement membrane molecules in vitro. To define the ultrastructural secreting pathway of these molecules, we immunolocalized heparan sulphate proteoglycan (HSPG) in ACC3 for 7 days of culture. In the early stage of culture, the main compartments immunolabelled were rough endoplasmic reticulum (rER) and small secretory vesicles. From days 3 to 4 after plating, it was noticed that HSPG was localized in partially dilated spaces of the perinuclear, rER and Golgi cisternae and in lysosomes or those fused with multivesicular bodies and endosomes. On and after day 5, almost every Golgi apparatus showed marked dilatation of the cisternae and HSPG was immunolocalized in these dilated spaces. In the later stage of culture, autophagic vacuoles or secondary lysosomes, which were simultaneously labelled for HSPG and cathepsin D, were accumulated in the cytoplasm. HSPG deposition in the intercellular space was clearly demonstrated from day 1 and increased during the culture. The results indicate that ACC3 cells have an enhanced turnover cycle for HSPG: not only its biosynthesis but also degradation of both endogenous or exogenous HSPG. Such intracellular events may be reflected in the characteristic histology and biological behaviour of adenoid cystic carcinomas.

Key words Adenoid cystic carcinoma · Heparan sulphate proteoglycan · Intracellular transport · Cryoultramicrotomy · Immunogold technique

T. Irié · J. Cheng · S. Kimura · R. Munakata · S. Taira · T. Saku (✉)
Department of Pathology, Niigata University School of Dentistry,
2–5274 Gakkocho-dori, Niigata 951, Japan
e-mail: tsaku@dent.niigata-u.ac.jp
Tel.: (+81)-25-223-6161, Fax: (+81)-25-223-9612

R. Munakata · S. Taira
Department of Oral and Maxillofacial Surgery,
Niigata University School of Dentistry, Niigata, Japan

Introduction

Adenoid cystic carcinoma is characterized histologically by a cribriform appearance resulting from formation of multi-pseudocystic spaces in each tumour cell nest. The pseudocysts are surrounded by tumour cells of the myoepithelial type and are filled with extracellular matrix components including basement membrane molecules [1–5]. Since there are few cellular components in the pseudocystic space, it has been postulated that these tumour cells secrete extracellular matrix components into the intercellular space [6–9]. The abundant retention of basement membrane molecules in the stromal space and pseudocystic cavities suggests that basement membrane-rich matrix is essential for proliferation of adenoid cystic carcinoma cells, and we have interpreted their frequent invasion of peripheral nerves, blood vessels, and skeletal muscles as showing that these carcinoma cells have an affinity to basement membranes [8]. Using the cell systems ACC2 and ACC3, [10, 11], we have also shown that adenoid cystic carcinoma cells attach, spread, and grow rapidly on matrices containing basement membrane molecules. These cell systems synthesize extracellular matrix molecules, secrete them into the extracellular milieu and remodel their extracellular deposits [11–14]; ACC2 cells form the characteristic pseudocystic space in three-dimensional collagen gel cultures and in transplants in SCID mice [15].

In the previous study [11], intracellular signals for the basement membrane molecules and fibronectin were distinguished from extracellular ones in ACC2 and ACC3 cells. In addition, we discriminated between two types of intracellular signals: rough endoplasmic reticulum (rER) and Golgi patterns. These interpretations were based solely on light microscopic observation, and we had no data on the subcellular localization of these molecules. We have meanwhile determined the subcellular immunolocalization of heparan sulphate proteoglycan (HSPG), one of the major basement membrane molecules, in ACC3 cells, because these cells synthesize HSPG most conspicuously among the basement membrane molecules

[11, 16]. We sought to confirm the intracellular secretory pathway of HSPG from biosynthesis to extracellular deposition by examining their ultrastructural appearances. We found ultrastructural evidence for the enhanced turnover of HSPG, which may be responsible for the characteristic histology and behaviour of adenoid cystic carcinomas.

Materials and methods

The ACC3 cell system was established from an adenoid cystic carcinoma arising in the parotid gland of a 49-year-old man [11, 17]. The cells were cultured in RPMI-1640 medium (Nissui Pharmaceutical Co., Tokyo, Japan) containing 15% fetal calf serum (Flow Laboratory, Irvine, UK), 1% glutamine (Nissui), 50 μg/ml streptomycin (Meiji Milk Products, Tokyo, Japan) and 50 IU/ml penicillin (Meiji) and incubated in a humidified 5% CO_2/95% air atmosphere at 37°C. For this experiment, ACC3 cells between passages 150 and 170 were used.

ACC3 cells were seeded at cell concentration of 1.3×10^4 in 2 ml complete medium in 35-mm plastic dishes, fed every 2 days with fresh medium, and incubated as described above. Cells were removed by trypsinization and counted for three sets of dishes every 24 h for 9 days.

Polyclonal antibodies against the bovine basement membrane type HSPG core protein were raised in rabbits as described elsewhere [8, 11, 18]. Rabbit polyclonal antibodies against rat cathepsin D [19] were used for identification of lysosomes. These polyclonal antibodies were purified by passage through columns of antigen-coupled Sepharose-4B (Pharmacia, Uppsala, Sweden). In immunocytochemical experiments, the antibodies were used at protein concentrations of 10–50 μg/ml. The second antibodies were colloidal gold-labelled goat anti-rabbit IgGs (gold particles: 5, 10 and 15 nm in diameter; 1:20 dilution; Amersham Life Science Products, Amersham, Bucks., UK).

For electron microscopy, ACC3 cells were seeded and fed as mentioned above. Each dish was fixed with 2.5% glutaraldehyde in 0.1 M phosphate buffer (pH 7.4) for 2 h on ice every 24 h for 9 days after plating and then postfixed in 2% osmium tetroxide in 0.1 M phosphate buffer (pH 7.4) for 2 h on ice. The dishes were dehydrated in graded ethanol series, and the cell layers were stripped off from plastic dishes with a rubber policeman. They were centrifuged for 10 min at 700×*g*, and then the pellets were embedded in Epon 812. Ultrathin sections were mounted on 150 mesh grids, stained with uranyl acetate and lead citrate, and examined by a Hitachi H-300 transmission electron microscope with an accelerating voltage of 75 kV.

For immunoelectron microscopy, dishes with the ACC3 cells seeded and incubated as described above were fixed with 4% paraformaldehyde and 0.5% glutaraldehyde in 0.1 M phosphate buffer (pH 7.4) for 2 h on ice every 24 h for 9 days after plating. The cell layers were stripped off from dishes with a rubber policeman after washing with 0.1 M phosphate buffer and were centrifuged as above. The pellets were cryoprotected with 20% polyvinyl pyrrolidone, 0.01 M sodium carbonate and 1.84 M sucrose in 0.1 M phosphate buffer (pH 7.4) overnight at 4°C and then frozen in liquid nitrogen. Ultrathin frozen sections were cut on a Reichert-Nissei Ultracut S equipped with a FC-S cryoattachment, as described elsewhere [18]. The sections were mounted on 150 mesh grids coated with Formvar and carbon.

For immunogold staining, all incubations were performed in a moist chamber at room temperature by floating grids on 20-μl droplets of reagents, basically according to the method of Goto et al. [20]. The grids were blocked with 3% normal goat serum in PBS for 15 min to prevent non-specific protein binding, then incubated with the primary antibodies for 1 h. After washing with PBS, the grids were incubated with colloidal gold (particles with a diameter of 10 nm)-labelled goat anti-rabbit IgG. For double staining, after the first immunostaining for HSPG using 5-nm gold particles, the grids were blocked with 3% normal goat serum in PBS containing 0.05 M glycine for 30 min. After washing with PBS, a second immunostaining for cathepsin D using 15 nm gold-labelled goat anti-rabbit IgG was performed by the same procedure as above. After incubation with the antibodies, the grids were postfixed with 2% glutaraldehyde and further with 1% osmium tetroxide. The grids were then stained with 2% uranyl acetate and embedded in a mixture of 3% polyvinyl alcohol (PVA) and 0.3% uranyl acetate (UA) with the UA/PVA ratio from 1:10 (positive counterstain) to 10:1 (negative counterstain), according to the method of Tokuyasu [21]. The grids were examined by a Hitachi H-300 electron microscope with an accelerating voltage of 75 kV.

Results

As shown in Fig. 1, ACC3 cells started logarithmic growth at 24 h after plating ($1.8\pm0.23\times10^4$) and continued until day 3 ($10.5\pm1.08\times10^4$), and then entered another, exponential, growth phase that persisted until day 8 ($2.1\pm0.20\times10^5$ at day 4, $3.8\pm0.43\times10^5$ at day 5, $6.4\pm0.46\times10^5$ at day 6, $1.09\pm0.058\times10^6$ at day 7, and $1.70\pm0.035\times10^6$ at day 8). The doubling time of ACC3 cells was about 36 h (Fig. 1).

When examined by electron microscopy on days 1–2 after seeding, ACC3 cells cultured on plastic dishes were seen to be hemispherical and to have plentiful microvilli with dilated ends at the apical surface. Their nuclei were large and irregularly lobulated. The cells spread widely and adhered tightly to the plastic surface with a number of microprojections on the basal plasma membrane (Fig. 2). There were many organelles including mitochondria and rough endoplasmic reticulum (rER) in the cytoplasm. In addition, several kinds of vacuolar structures were noticeable: they were round dilated cisternae of the rER (Fig. 3a), large spherical vacuoles containing slightly electron-dense homogeneous material, and smaller secretory granules or lysosomes along the basolateral surface (Fig. 2). Free ribosomes and polyribosomes were abundant in the cytoplasm (Fig. 3a). On the ultrathin cryosections made on the same days, perinuclear and rER cisternal spaces were immunolabelled with gold particles, indicating the localization of HSPG core protein. Gold particles for HSPG were also localized in amorphous or fibrillar material with a rather low electron

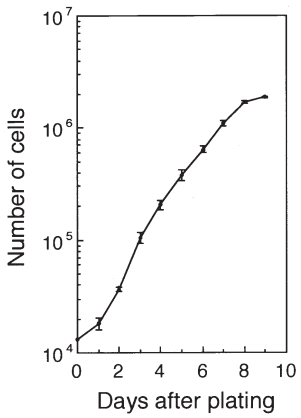

Fig. 1 Growth curve of ACC3 cells

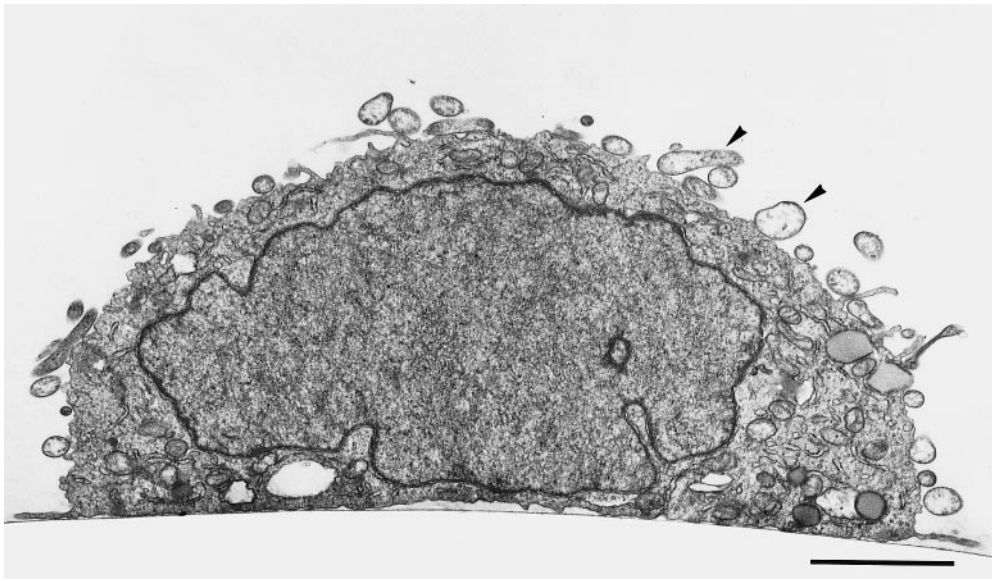

Fig. 2 Electron micrograph of ACC3 cell at day 1 in resin section. ACC3 cell shows hemispheric shapes in vertical section and plentiful microvilli with dilated ends (*arrowheads*) at the apical surface. It has a large and irregularly lobulated nucleus and contains many organelles, such as mitochondria and rough endoplasmic reticulum (*rER*), lipid droplets and many kinds of vesicles. ×11,000; *bar* 2 μm

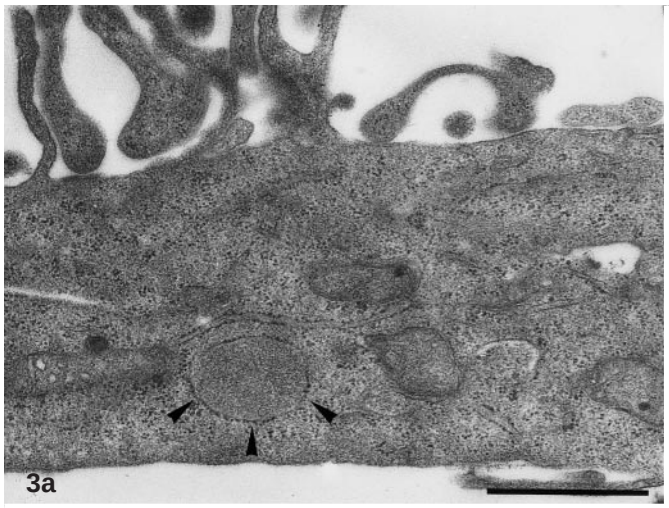

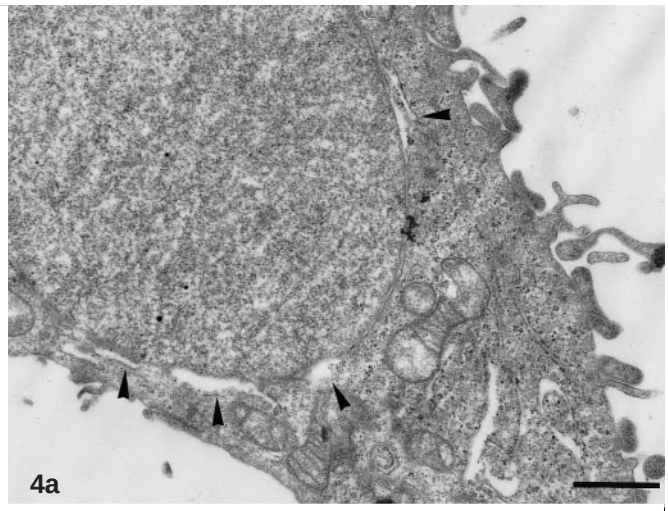

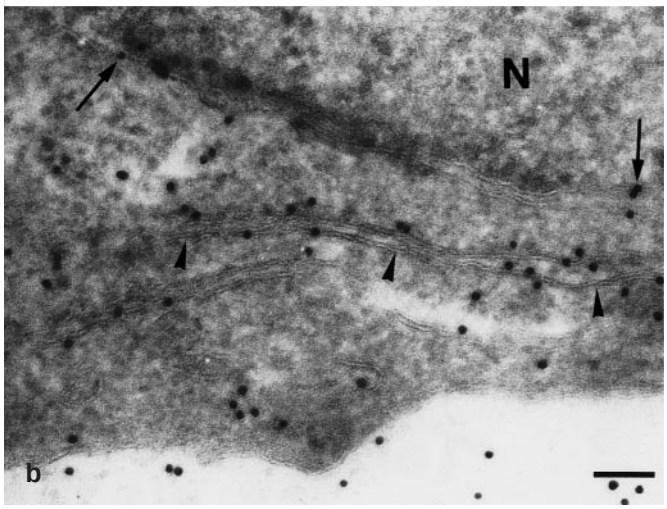

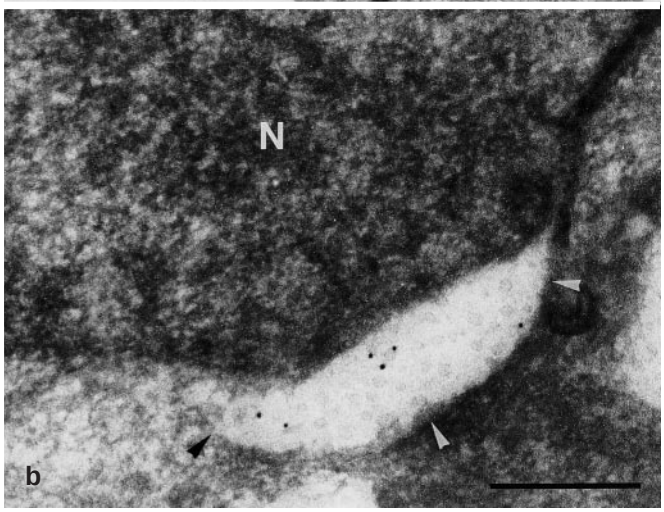

Fig. 3 ACC3 cell at day 2 in **a** resin section and **b** cryosection immunolabelled for heparan sulfate proteoglycan (HSPG). **a** ACC3 cell shows round dilatation of rER (*arrowheads*). Free ribosomes or polyribosomes are also abundant in the cytoplasm. ×21,000; *bar* 1 μm. **b** Gold particles for HSPG are localized in rER (*arrowheads*) and perinuclear space (*arrows*) and are also confined in amorphous or fibrillar material in extracellular space (*N* nucleus). ×74,000; *bar* 0.1 μm

Fig. 4 ACC3 cell at day 3 in **a** resin section and **b** cryosection immunolabelled for HSPG. **a** Dilatation of perinuclear space (*arrowheads*) is frequently observed. ×11,000; *bar* 1 μm. **b** Gold particles for HSPG are accumulated in dilated perinuclear space (*arrowheads*) (*N* nucleus). ×39,000; *bar* 0.5 μm

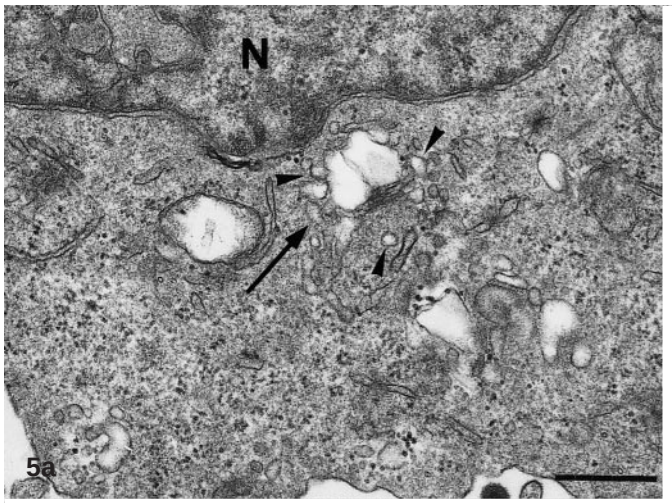

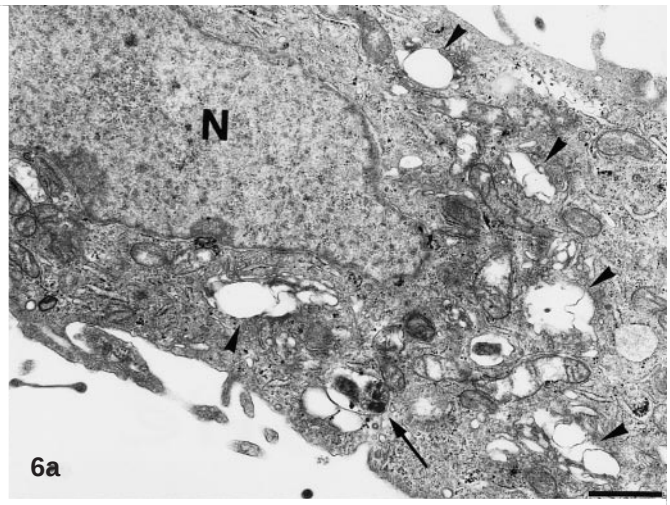

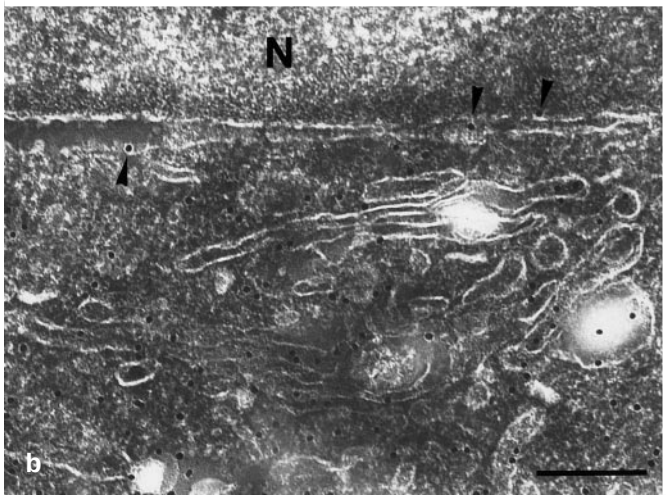

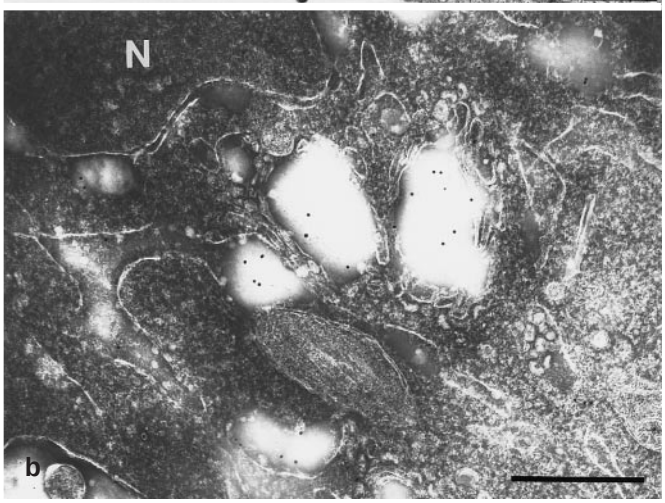

Fig. 5 ACC3 cell at day 4 in **a** resin section and **b** cryosection immunolabelled for HSPG. **a** Dilated cisternae are conspicuous in Golgi apparatus (*arrow*) in perinuclear area, where there are many Golgi vesicles or small tubulovesicular structures (*arrowheads*). ×27,000; *bar* 0.5 μm **b** Many gold particles for HSPG are localized in dilated Golgi cisternae in addition to rER cisternae, perinuclear space (*arrowheads*) and numerous tubulovesicular structures (*N* nucleus). ×70,000; bar 0.2 μm

Fig. 6 ACC3 cell at day 5 in **a** resin section and **b** cryosection immunolabeled for HSPG. **a** Every Golgi apparatus (*arrowheads*) shows marked dilatation of its cisternae; round-shaped dilatation of rER cisternae and autophagic vacuoles (*arrow*) are noticeable. ×10,000; *bar* 1 μm. **b** Markedly dilated Golgi cisternae contain gold particles for HSPG (*N* nucleus). ×35,000; *bar* 0.5 μm

density in the extracellular space of the basal side of cells (Fig. 3b). Extracellular deposition of HSPG was first recognized at the basal side of ACC3 cells from day 1, and thereafter its extracellular signals at the basolateral aspect increased in number.

After 3 days of culture, focal dilatation of the perinuclear space was noticeable (Fig. 4a). The space contained many gold particles of HSPG (Fig. 4b). At day 4, Golgi cisternae became partially dilated, and these irregularly-shaped rER and Golgi apparatus were surrounded by Golgi vesicles and small tubulovesicular structures (Fig. 5a). On the cryosections, a large number of gold particles of HSPG were seen in the Golgi cisternae and in numerous small vesicles (Fig. 5b), discernible only by negative counterstaining around them. Gold particles of HSPG found in the perinuclear and rER cisternal space decreased in number after the first 3 days.

On day 5, almost every Golgi apparatus had markedly dilated cisternae with electron-lucent contents (Fig. 6a). Focal and round dilation of cisternae was still seen in the rER. There were various-sized vacuoles (0.7 μm in diameter at the largest) with heterogeneous contents, which were regarded as autophagic secondary lysosomes. On the cryosections, markedly dilated Golgi cisternae similar to those shown in Fig. 6a contained gold particles of HSPG (Fig. 6b). Gold particles of HSPG were also found in phagosomes as well as in the dilated rER cisternal space. Large spherical vacuoles (1–2 μm in diameter) with low electron-dense contents, first seen at day 4, increased in number (Fig. 7a). They were considered to be secondary lysosomes because of the presence of myelin-like structures in the lumina. In addition, there were small multivesicular bodies (0.5 μm in diameter) around focally dilated rER and the Golgi cisternae. On

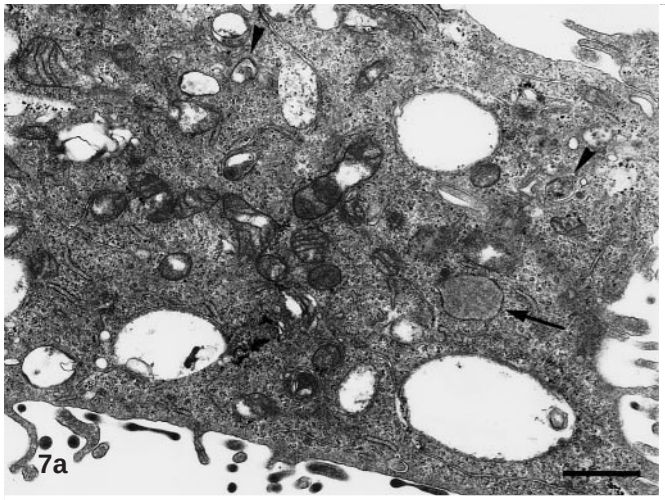

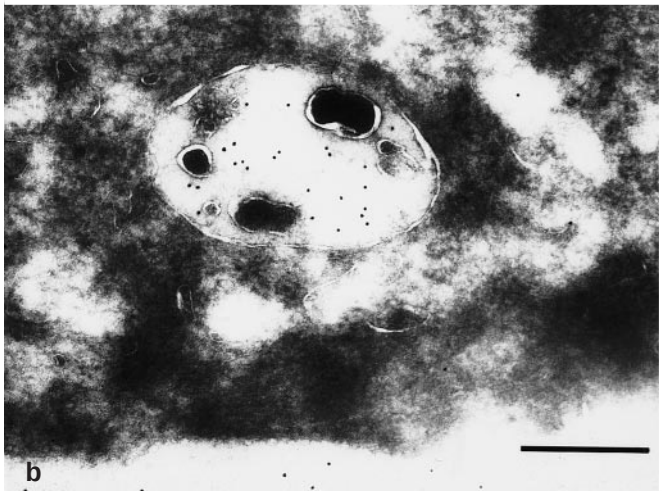

Fig. 7 ACC3 cell at day 5 in **a** resin section and **b** cryosection immunolabelled for HSPG. **a** Large distended vacuoles usually contain low electron-dense material, but sometimes myelin bodies. Multivesicular bodies (*arrowheads*) are scattered among these vacuoles and rER with dilated cisternae (*arrow*). ×10,000; *bar* 1 μm **b** Large spherical vacuoles contain numerous gold particles for HSPG, which are confined to electron-lucent amorphous material. ×34,000; *bar* 0.5 μm

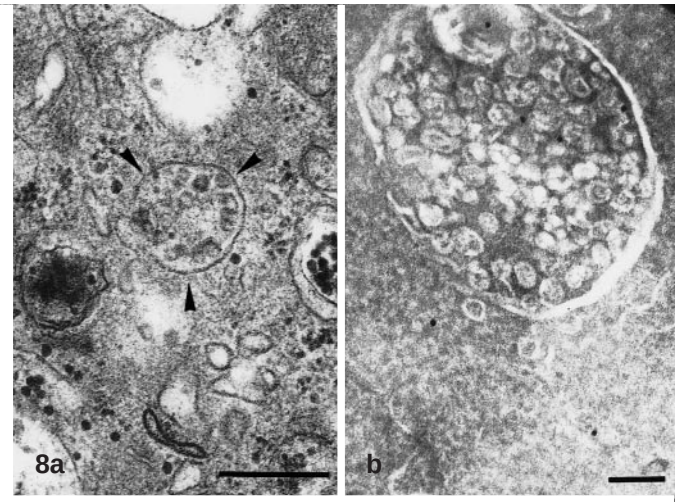

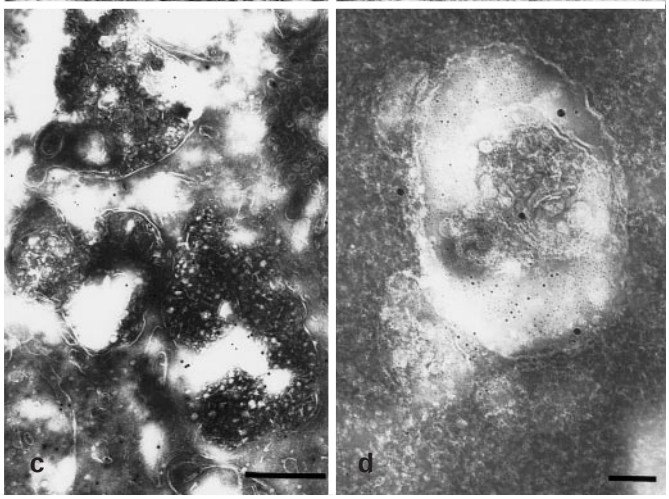

Fig. 8 Multivesicular bodies and autophagic vacuoles in ACC3 cell at day 5 **a** in resin sections and **b–d** in cryosections immunolabelled **b** for cathepsin D, **c** for HSPG and **d** for HSPG and cathepsin D. **a** Multivesicular body (*arrowheads*) is apparently limited by unit membrane and contains numerous vesicles. ×40,000; *bar* 0.3 μm **b** Multivesicular body contains gold particles for cathepsin D. ×70,000; *bar* 0.1 μm **c** Autophagic vacuoles fused with multivesicular bodies contain heterogeneous material such as membranous fragments and myelin bodies. These vacuoles contains gold particles for HSPG. ×20,000; *bar* 0.5 μm **d** Autophagic vacuoles contain gold particles for both HSPG (5 nm gold) and cathepsin D (15 nm gold). ×60,000; *bar* 0.1 μm

the cryosections, large spherical vacuoles (1–2 μm in diameter) contained numerous gold particles of HSPG (Fig. 7b). Within the vacuolar space, the gold particles of HSPG were confined in fine and faintly electron-dense granules or in somewhat fibrillar material. Also in the extracellular space, the gold particles of HSPG were localized in the similar granulo-fibrillar material. The characteristic multivesicular bodies (0.5 μm in diameter) mentioned above were apparently membrane limited and contained numerous small vesicles with homogeneous appearances (0.05 μm in diameter; Fig. 8a). These bodies appeared more often in confluent cultures. On cryosection, they contained gold particles for cathepsin D (Fig. 8b), indicating that cathepsin D is transported into multivesicular bodies via the Golgi apparatus and that multivesicular bodies function as a sort of primary lysosomes. In connection with the multivesicular bodies, there were larger HSPG-immunopositive vacuoles (0.5–1.0 μm in diameter), with heterogeneous contents such as membranous fragments forming myelin figures and small vesicles/granules (0.05 μm in diameter). We suggest that these were autophagosomes or secondary lysosomes fused with multivesicular bodies (Fig. 8c). These hybrid vacuoles were simultaneously immunolabelled with 5-nm gold particles for HSPG and 15-nm gold particles for cathepsin D (Fig. 8d).

At day 3 of culture and thereafter, intercellular canaliculus-like structures began to appear among the ACC3 cells. These were formed by the sealing of plasma membranes of neighbouring cells with desmosomes and with tight junctions. Some of the microvilli with actin fila-

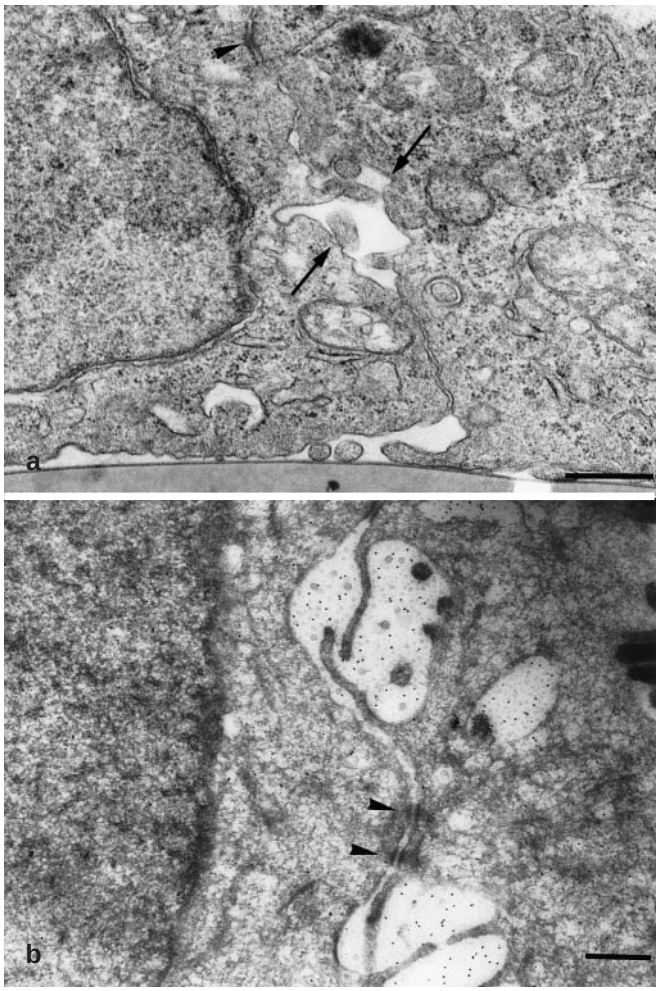

Fig. 9 Intercellular adhesion of ACC3 cells at day 4 **a** in resin section and **b** cryosection immunolabelled for HSPG. **a** Intercellular canaliculus (*arrows*) is formed by sealing of plasma membranes of neighbouring cells with desmosomes (*arrowheads*) and by tight junctions. Microvilli projecting into lumen contain actin filament cores. ×23,000; *bar* 0.5 μm **b** Gold particles are accumulated in intercellular canaliculi and in intracellular vacuoles around canaliculi. ×17,000; *bar* 0.5 μm

ment cores were projecting into the lumina (Fig. 9a). On cryosection, HSPG labelling was limited to faintly electron-dense granules or to similar electron-dense amorphous material within particular intercellular spaces (Fig. 9b). These intercellular substances resembled the ultrastructural features of the vacuolar contents shown in Fig. 7a and b. Surrounding these structures were vacuoles (0.5–0.8 μm in diameter) containing gold particles for HSPG in the cytoplasm.

Discussion

The primary aim of the present study was to clarify the sequential transition of subcellular localization of HSPG in ACC3 cells, using cryoultramicrotomy [18, 22] since HSPG is not well immunolocalized on resin sections by the post-embedding method [18, 19]. Its other important advantage was negative counterstaining on ultrathin frozen sections, enabling us to recognize numerous vesicular structures that are masked in positive electron stained sections [23]. Freezing pellets of scraped cells was our own device for screening many cells efficiently.

The present study shows that our interpretations of the intracellular and extracellular immunofluorescence signals of HSPG in ACC3 cells were not always accurate in terms of location. In the immunofluorescence study [11], we suggested that the intracellular signals, with diffuse and fine granular patterns, were evidence of biosynthesis of HSPG in the rER (ER pattern) and that the perinuclear aggregation of coarse granular signals was evidence of transport of HSPG into the Golgi apparatus (Golgi pattern). Dotted or thread-like signals in the extracellular space represented intercellular deposition of HSPG. This study revealed that the ER pattern of immunofluorescence was identical to the accumulation of gold particles for HSPG core protein in the rER cisternae, indicating that the biosynthesis of HSPG is actively occurring in the cells. The Golgi pattern of immunofluorescence is HSPG retention within the Golgi stacks. However, the dilated perinuclear spaces seen in the middle stage of culture represent another Golgi pattern and were quite characteristic of ACC3 cells. The presence of irregularly dilated rER and Golgi cisternae suggests an enhanced synthetic cycle or overproduction of HSPG molecules not seen in other carcinomas. Similar observations have been obtained when lysosomal enzymes are inhibited with leupeptin, vinblastine, and chloroquine in hepatocytes [24–26], or when proteoglycan secretion was inhibited with monensin [27]. The secretory process of newly synthesized HSPG may be regulated by a lysosomal degrading mechanism, which takes care of overproduction of the molecule. Therefore, loss of control of such a cycle of degradation may be one of the reasons for the overproduction of HSPG, and this overproduction may result in the characteristic histology of adenoid cystic carcinoma.

The most interesting finding in the present study was the localization of HSPG in several kinds of vesiculovacuolar structures other than focal dilatations of rER and Golgi cisternae. These vesiculo-vacuolar structures were roughly classified into small round transport or secretory vesicles (ca. 0.2 μm diameter) budded from the rER to the Golgi apparatus or from there to the cell surface, larger late-endosomal vesicles (0.5–1.0 μm diameter) fused with lysosomes, lysosomal vacuoles (0.5–1.0 μm diameter) fused with multivesicular bodies, and the largest, spherical vacuoles (1–2 μm diameter) of a kind of autophagosomes. Since the last three were simultaneously immunolabelled for cathepsin D and HSPG, they are thought to take part in the degradation of HSPG. These findings suggest that there is an extraordinary variety of HSPG-degrading processes in ACC3 cells. Since increased numbers of autophagosomes are characteristic of cells in mucopolysaccharidoses (MPS), including MPS III type A, which lacks heparan sulphate

lyases [28], further examination is necessary to determine whether ACC3 cells are able to degrade HSPG in their lysosomes.

Classical explanations of intracellular transport [29] suggest the HSPG molecules in lysosomal compartments can be regarded as being in a degradation pathway, starting from endocytosis. For the present, our findings are evidence that ACC3 cells themselves participate directly in remodelling HSPG deposits in the extracellular milieu. Another possible explanation for the localization of HSPG molecules in lysosomes is that they are in their biosynthetic pathway directly from the rER or Golgi apparatus. Such degradation systems for newly synthesized proteins have been demonstrated in type I collagen in fibroblasts [30] or aminopeptidase N in enterocytes [31]. It is uncertain which intracellular compartments are responsible. Several groups of researchers have suggested that lysosomes are involved in this process [30, 32, 33], although conflicting evidence of extralysosomal degradation of newly synthesized collagen has also been presented [34–36].

The extracellular immunofluorescence for HSPG was only recognized in the later stage of culture as dotted or thread-like patterns [11]. In the present study, however, we demonstrated immunogold signals for HSPG in the extracellular space even 24 h after plating. This may be due to higher resolution or sensitivity of the technique of immunoelectron microscopy. We have already demonstrated that a discernible bulk of HSPG molecules is shed by ACC3 cells into the culture medium within 3 h after plating, in a pulse-chase experiment using ^{3}H-leucine/^{35}S-methionine labelling [37]. The accumulation of gold particles for HSPG in intercellular canaliculus-like structures may correspond to the dot- or thread-like immunofluorescence along the cell border. The localization of HSPG in the canalicular space is not always consistent with the primary function of intercellular canaliculi [38], because this type of HSPG is an extracellular matrix molecule. Functional differentiation may not necessarily be in agreement with the morphological architectures of ACC3 cells. True ductal structures are rarely formed within adenoid cystic carcinoma; these are mostly composed of cells with myoepithelial characteristics [5], and some hybrid of stromal pseudocysts and ductal lumina might be represented in the intercellular canaliculi of ACC3 cells in culture.

Acknowledgement This work was supported in part by Grants-in-Aid for Scientific Research from the Ministry of Education, Science, Sports and Culture, Japan.

References

1. Toida M, Takeuchi J, Hara K (1984) Histochemical studies of intercellular components of salivary gland tumors with special reference to glycosaminoglycan, laminin and vascular elements. Virchows Arch [A] 403:15–26
2. Toida M, Takeuchi J, Sobue M (1985) Histochemical studies on pseudocysts in adenoid cystic carcinoma of the human salivary gland. Histochem J 17:913–924
3. Caselitz J, Schulzei G (1986) Adenoid cystic carcinoma of the salivary glands: an immunohistochemical study. J Oral Pathol 5:308–318
4. Azumi N, Battiforah H (1987) The cellular composition of adenoid cystic carcinoma. An immunohistochemical study. Cancer 60:1589-1598
5. Saku T, Okabe H, Yagi Y, Sato E, Tsuda N (1984) A comparative study on the immunolocalization of keratin and myosin in salivary gland tumors. Acta Pathol Jpn 4:1031–1040
6. Busuttil A (1977) Adenoid cystic carcinoma of the minor salivary glands. J Laryngol Otol 91:41–53
7. Mochomovitz L E, Kahn L B (1977) Adenoid cystic carcinoma of the salivary gland and its histologic variants. Oral Surg Oral Med Oral Pathol 44:394–404
8. Cheng J, Saku T, Okabe H, Furthmayr H (1992) Basement membranes in adenoid cystic carcinoma: an immunohistochemical study. Cancer 69:2631–2640
9. Hübner G, Kleinsasser O, Klein H (1969) Zur Feinstruktur und Genese der Cylindrome der Speicheldrusen. Virchows Arch [A] 347:296–315
10. Shibata Y, Cheng J, Saku T, Okabe H (1993) Proliferation of adenoid cystic carcinoma cells controlled by extracellular matrix. Jpn J Oral Biol 35:169
11. Cheng J, Irié T, Munakata R, Kimura S, Nakamura H, He RG, Liu AR, Saku T (1995) Biosynthesis of basement membrane molecules by salivary adenoid cystic carcinoma cells: an immunofluorescence and confocal microscopic study. Virchows Arch 426:577–586
12. Sobue M, Takeuchi J, Niwa M, Yasui C, Nakagaki S, Nagasaka T, Fukatsu T, Saga S, Nakashima N (1989) Establishment of a cell line producing basement membrane components from an adenoid cystic carcinoma of the human salivary gland. Virchows Arch [A] 57:203–208
13. Shirasuna K, Watatani K, Furusawa H, Saka M, Morioka S, Yoshioka H, Matsuya T (1990) Biological characterization of pseudocyst-forming cell lines from human adenoid cystic carcinomas of minor salivary gland origin. Cancer Res 50: 4139–4145
14. Shirasuna K, Saka M, Hayashido Y, Yoshioka H, Sugiura T, Matsuya T (1993) Extracellular matrix production and degradation by adenoid cystic carcinoma cells: participation of plasminogen activator and its inhibitor in matrix degradation. Cancer Res 53:147–152
15. Munakata R, Irié T, Cheng J, Nakajima T, Saku T (1996) Pseudocyst formation by adenoid cystic carcinoma cells in collagen gel culture and SCID mice. J Oral Pathol Med 25: 441–448
16. Kimura S, Toyoshima K, Cheng J, Oda K, Saku T (1994) Basement membrane heparan sulfate proteoglycan synthesized by ACC3, adenoid cystic carcinoma cells of the human salivary gland origin. Trans Soc Pathol Jpn 83:171
17. He RG, Zhang XS, Zhou XJ (1988) The establishment of cell lines of adenoid cystic carcinoma of human salivary glands (ACC2, ACC3) and a study of morphology. West Chin J Stomatol 6:1–4
18. Saku T, Furthmayer H (1989) Characterization of the major heparan sulfate proteoglycan secreted by bovine aortic endothelial cells in culture. J Biol Chem 264:3514–3523
19. Saku T, Sakai H, Shibata Y, Kato Y, Yamamoto K (1991) An immunocytochemical study on distinct Intracellular localization of cathepsin E and cathepsin D in human gastric cells and various rat cells. J Biochem 110:956–964
20. Goto M, Meyermann R, Wekerle H (1987) Ultrastructural immunocytochemistry of glia cells: double labeling studies using LR White embedding and colloidal gold. Histochemistry 87:201–207
21. Tokuyasu KT (1989) Use of poly(vinylpyrrolidone) and poly(vinyl alcohol) for cryoultramicrotomy. Histochem J 21: 163–171
22. Griffiths G, Simons K, Warren G, Tokuyasu KT (1986) Immunoelectron microscopy using thin frozen sections: application to studies of the intracellular transport of Semliki forest virus spike glycoproteins. Methods Enzymol 96:466–483

23. Fujimoto T, Nakade S, Miyawaki A (1992) Localization of inositol 1,4,5-triphosphate receptor-like protein in plasmalemmal caveolae. J Cell Biol 119:1507–1513
24. Furuno K, Ishikawa T, Kato K (1982) Appearance of autolysosomes in rat liver after leupeptin treatment. J Biochem 91:1485–1494
25. Henell F, Glaumann H (1984) Effect of leupeptin on the autophagic vacuolar system of rat hepatocytes: correlation between ultrastructure and degradation of membrane and cytosolic proteins. Lab Invest 51:46–56
26. Glaumann H, Ahlberg J (1987) Comparison of different autophagic vacuoles with regard to ultrastructure, enzymatic composition, and degradation capacity–Formation of crinosomes. Exp Mol Pathol 47:346–362
27. Patcliffe A, Fryer PR, Hardingham TE (1985) Proteoglycan biosynthesis in chondrocytes: protein A-gold localization of proteoglycan protein core and chondroitin sulfate within Golgi subcompartments. J Cell Biol 101:2355–2365
28. Resnick JM, Whitley CB, Leonard AS, Krivit W, Snover DC (1994) Light and electron microscopic features of the liver in mucopolysaccharidosis. Hum Pathol 25:276–286
29. Alberts B, Bray D, Lewis J, Raff M, Roberts K, Watson JD (1994) Molecular biology of the cell, 3rd edn. Garland, New York, pp 599–633
30. Ripley CR, Fant J, Bienkowski RS (1993) Brefeldin A inhibits degradation as well as production and secretion of collagen in human lung fibroblast. J Biol Chem 268:3677–3682
31. Hansen GH, Danielsen EM, Sjöström H, Norén O (1989) Organelles involved in the intracellular transport of newly synthesized aminopeptidase N and their acidity. Eur J Cell Biol 49:154–161
32. Smith RE, Farquhar MG (1966) Lysosome function in the regulation of the secretory process in cells of the anterior pituitary gland. J Cell Biol 31:319–347
33. Berg RC, Schwartz ML, Crystal RG (1980) Regulation of the production of secretory protein: Intracellular degradation of newly synthesized “defective” collagen. Proc Natl Acad Sci USA 77:4746–4750
34. Leblond CP (1989) Synthesis and secretion of collagen by cells of connective tissue, bone, and dentin. Anat Rec 224: 123–138
35. Bienkowski RS, Pipley CR, Gitzelmann R, Steinmann B (1990) Collagen degradation in I-cells is normal. Biochem Biophys Res Commun 168:479–484
36. Barile FA, Guzowski DE, Ripley C, Siddigi ZA, Bienkowski RS (1990) Ammonium chloride inhibits basal degradation of newly synthesized collagen in human fetal lung fibroblast. Arch Biochem Biophys 276:125–131
37. Kimura S, Koyano Y, Cheng J, Saku T (1996) Turnover of basement membrane heparan sulphate proteoglycan in salivary adenoid cystic carcinoma cells. Trans Soc Pathol Jpn 85:273
38. Junqueira LC, Carneiro J, Kelley RO (1995) Basic histology, 8th edn. Appleton & Lange, Norwalk, pp 314–324